

EFFECT OF ANNEALING TEMPERATURE ON THE MICROSTRUCTURE AND HARDNESS OF Fe-Mn-Si-Cr-Ni-Co SHAPE MEMORY ALLOY PROCESSED BY WIRE DRAWING¹

Elaine Cristina Andrade²
Heide Heloise Bernardi³
Leonardo Kenji Fudo Naito⁴
Jorge Otubo⁵

Abstract

Stainless shape memory alloys (SMA's) have been studied since the 90's. The Fe-Mn-Si-Cr-Ni-Co SMA used in this work was processed by wire drawing varying the area reductions, AR's (14%, 39% and 57%) and annealing temperature from 350°C to 1050°C during 1 hour. The microstructural characterization was performed by optical microscopy (OM), scanning electron microscopy (SEM) and Vickers hardness testing. The results showed that the increase of area reduction promoted increase in hardness for the cold drawn and annealed conditions. Results show that the precipitation became noticeable at 450°C and 550°C for samples with AR=39% and 57%, respectively.

Key words: Stainless SMA; Wire drawing; Annealing; Hardness testing.

¹ Technical contribution to 67th ABM International Congress, July, 31th to August 3rd, 2012, Rio de Janeiro, RJ, Brazil.

² Master's student (Instituto Tecnológico de Aeronáutica, ITA).

³ Pos doctoral fellow (Instituto Tecnológico de Aeronáutica, ITA).

⁴ Master's student (Instituto Tecnológico de Aeronáutica, ITA).

⁵ Professor (Instituto Tecnológico de Aeronáutica, ITA).

1 INTRODUCTION

2

According to Wen et al.⁽¹⁾ Fe-Mn-Si shape memory alloys (SMA) have received a special attention in the past 30 years since the discovery of the shape memory effect (SME) in 1982 by Sato. In the 90's they were started the development of stainless SMA as an alternative to the Ti-Ni SMA's due to the low cost, good corrosion resistance, good workability and good weldability.⁽²⁻⁷⁾ The shape memory effect (SME) in these alloys is related to the martensitic transformation $\gamma(\text{FCC}) \leftrightarrow \varepsilon(\text{HCP})$,⁽⁸⁻¹²⁾ which is affected by some factors, such as the alloying elements,^(1,2,5,8) annealing treatment^(3,8,13) deformation temperature, pre-strain level and thermomechanical training.^(1-3,5,8,13) Among these parameters, the annealing treatment is the more effective in the control of SME in Fe-Mn-Si-Cr-Ni based alloys.⁽⁸⁾ Some variations in annealing conditions promote microstructural changes in the parent phase, influencing the SME.

The SME is also improved by the presence of some defects, such as Shockley partial dislocations, stacking faults and grain boundaries. These defects function as a nucleation site for $\gamma \rightarrow \varepsilon$ martensitic transformation.^(8,13) It has been shown that the increase in the annealing temperature increases the grain size leading to the degradation of SME. This occurs because the larger the grain size, larger will be the distance that the Shockley partial dislocation should move through from one boundary to another, executing the forward and backward $\gamma \leftrightarrow \varepsilon$ transformation.^(5,10) When the grain size is small this distance becomes smaller making the $\gamma \leftrightarrow \varepsilon$ transformation easier and therefore the SME is improved.

Various deformation techniques have been applied to produce grain refinement in the microstructure such as forging, rolling and cold drawing.^(1,11,14) The degree of area reduction is an effective parameter in the control of the nucleation rate and grain growth during the annealing step.^(15,16) The aim of this paper is to evaluate the influence of area reductions in the microstructural evolution and hardness during the annealing in different temperatures of the Fe-Mn-Si-Cr-Ni-Co stainless SMA processed by wire drawing.

3 EXPERIMENTAL PROCEDURES

The chemical composition of Fe-Mn-Si-Cr-Ni-Co stainless SMA used in this work is shown in Table 1. The starting vacuum induction melted ingot of 65 x 65 mm² was hot forged down to 20 x 20 mm² and then hot rolled down to 6.75 x 6.75 mm² corner rounded bar. Then the bar was cold drawn to 2.38 mm intercalating continuous annealing step of 1050°C. Finally the wire was solution treated at 1050°C during 30 min and then water quenched to room temperature. The ingot fabrication and thermomechanical processing up to this stage can be seen elsewhere.⁽¹⁷⁾ The 2.38 mm in diameter wire was cold drawn to a final diameter of 1.56 mm adjusting the intermediate annealing at 2.004 mm (AR=39%), and 1.704 mm (AR=14%). The 57% area reduction wire was obtained drawing directly from 2.38mm wire.

Table 1. Chemical composition (% wt.) of stainless SMA

Fe	Mn	Si	Cr	Ni	Co	C	S	P
balance	7.79	5.11	13.04	5.90	11.90	0.044	<0.003	0.007

The wires with different area reductions were annealed in a box furnace at temperatures varying from 350°C to 1050°C during 1 hour and then cooled in air. The microstructural characterization of solution treated wire, cold drawn wires and annealed wires were done using a Carl Zeiss optical microscope (OM) coupled with CCD camera and FEI Quanta 400 scanning electronic microscope (SEM). Vickers hardness testing was performed in the longitudinal section of the specimens using a FM-700 microindenter with setting the load to 200gf during 10s.

4 RESULTS

5

The microstructure of solution treated sample at 2.38 mm is shown in Figure 1.

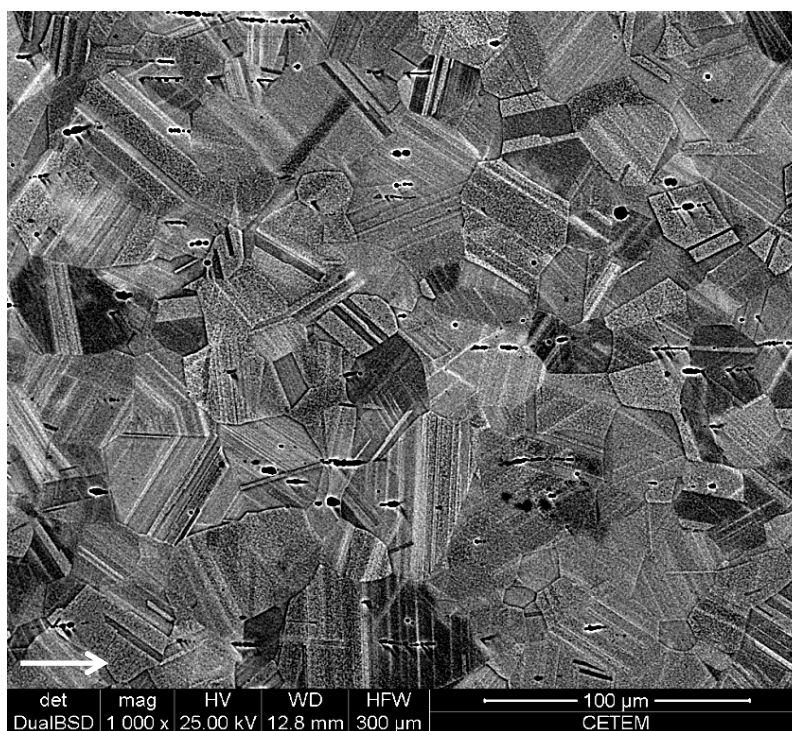


Figure 1. Longitudinal section microstructure of the solution treated at 1050°C during 30 min and 2.38 mm in diameter wire. (SEM-BSE). The white arrow indicates the wire drawing direction.

The microstructure of as drawn conditions wires with area reductions of 14%, 39% and 57%, and annealed conditions at 450°C, 550°C, 750°C, 850°C and 950°C during 1 hour are shown in Figure 2, Figure 3 and Figure 4 respectively.

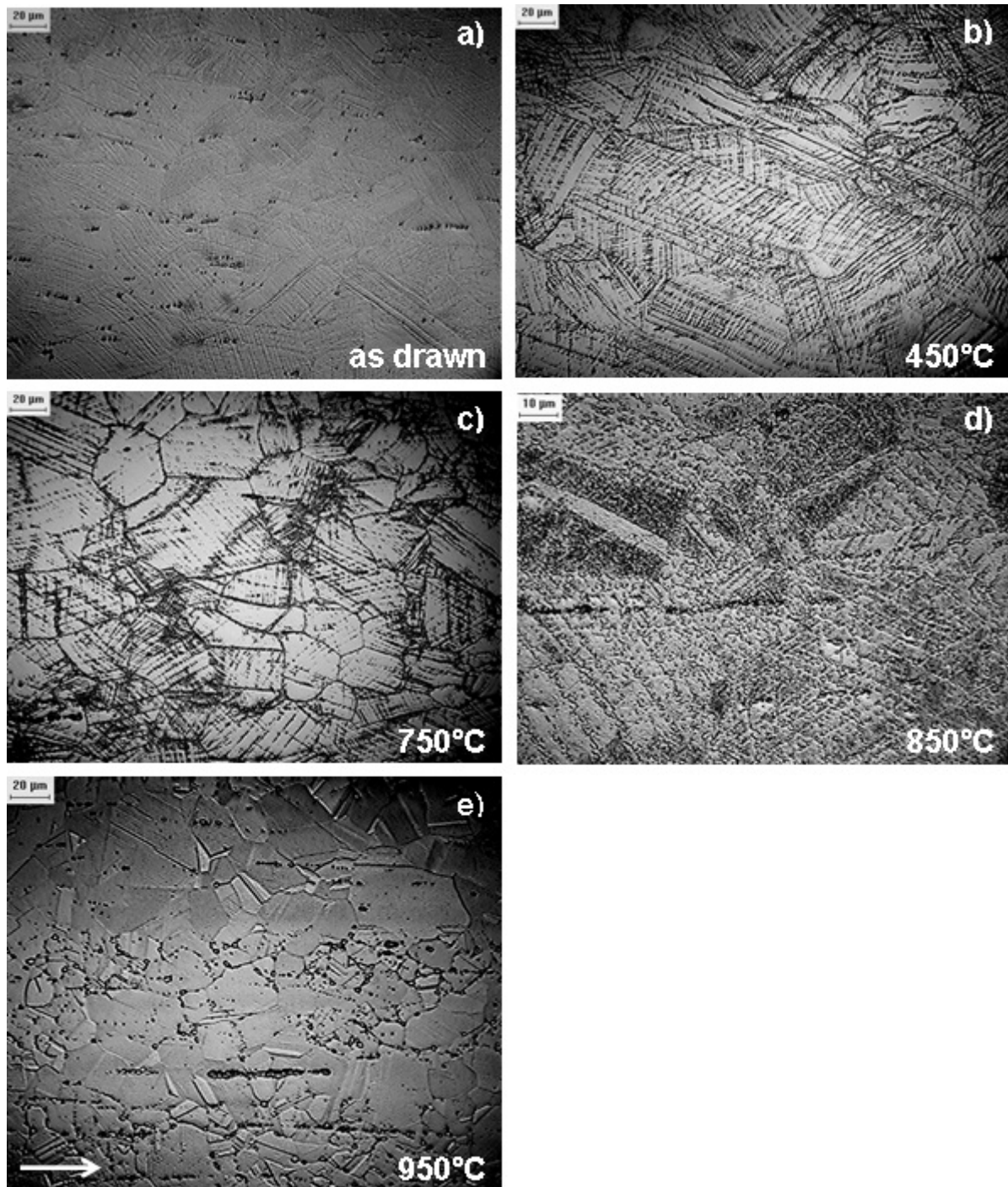


Figure 2. Microstructure of the wire samples with area reduction of 14% in different conditions: (a) as drawn, annealed at (b) 450°C, (c) 750°C, (d) 850°C and (e) 950°C. The white arrow indicates the wire drawing direction.

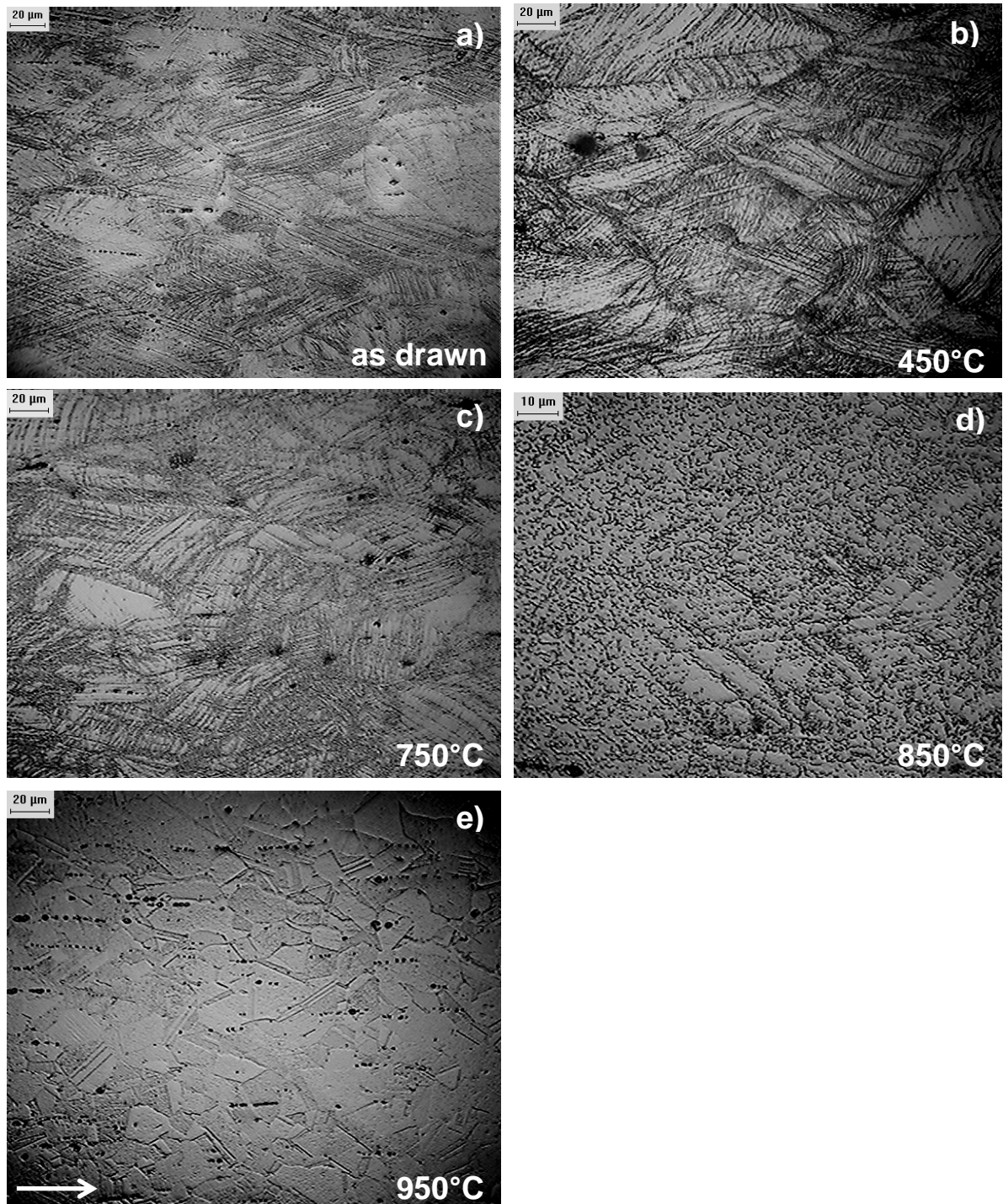


Figure 3. Microstructure of the wire samples with area reduction of 39% in different conditions: (a) as drawn, annealed at (b) 450°C, (c) 750°C, (d) 850°C and (e) 950°C. The white arrow indicates the wire drawing direction.

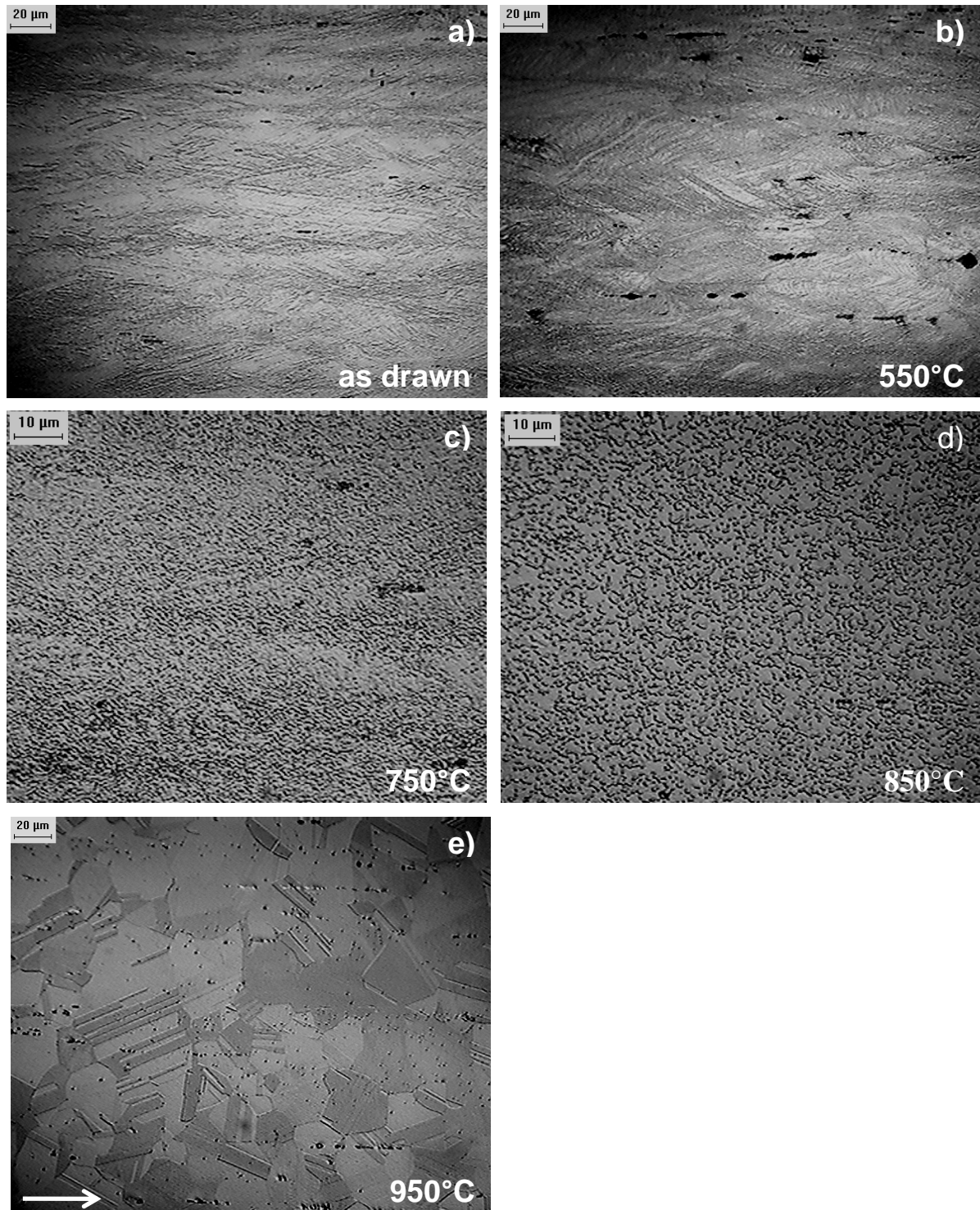


Figure 4. Microstructure of the wire samples with area reduction of 57% in different conditions: (a) as drawn, annealed at (b) 550°C, (c) 750°C, (d) 850°C and (e) 950°C. The white arrow indicates the wire drawing direction.

Figure 5 presents the results of hardness values for the samples in as drawn condition and after annealing in different temperatures from 350°C to 1050°C. For comparison purpose it is shown the hardness values of solution treated samples and then annealed in the same condition of as drawn samples.

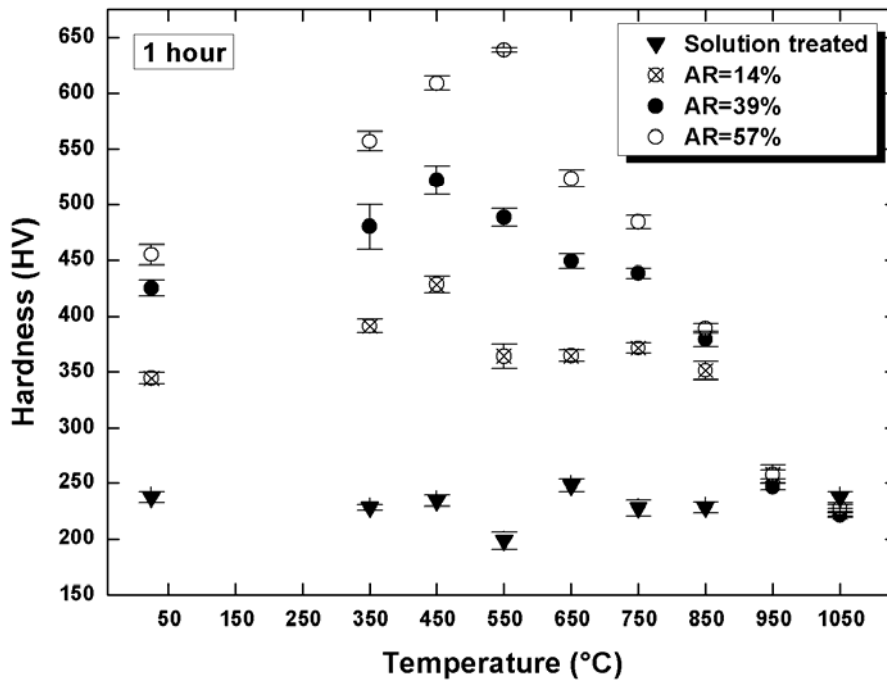


Figure 5. Effect of annealing temperature on the hardness of the Fe-Mn-Si-Cr-Ni-Co alloy wires subjected to 14%, 39% and 57% area reduction respectively.

6 DISCUSSION

It is observed in the microstructure of the solution treated sample (Figure 1) the presence of annealing twins, which are characteristic defects of Fe-Mn-Si based SMA's, that have a low stacking fault energy (SFE).^(11,13,18) The effects of increasing the area reductions for as drawn wires are shown in Figure 2a, Figure 3a and Figure 4a. The texture alignment in the drawing directions (horizontal direction of the pictures) increases as the area reduction increases. In Figure 2a one can still see the slip bands and grain boundaries but not in Figure 4a. The Figure 3a shows heterogeneous deformation probably related to favorable preferential orientation on the drawing direction. The cumulative work hardening seen in the microstructure of Figures 2a, 3a and 4a is corroborated with hardness increase shown in Figure 5. The hardness increase from about 237 HV of solution treated sample to a maximum of 455 HV for AR=57%, that is almost twice. It is well known that the larger the cold work more and more crystallographic defects are created in microstructure (i.e. grain boundaries, dislocations tangles, stacking faults and vacancy clusters); which increase the internal energy, raising the strength of material.

As seen in Figure 5, the solution treated sample does not present hardening effect after heat treatment from 350°C to 1050°C compared to drawn wires with variable area reduction. All the drawn wires had their hardness increased after heat treatment being the effect larger the larger is the area reductions. All the samples presented a maximum in hardness being 428HV at 450°C, 522HV at 450°C and 639HV at 550°C respectively for AR=14%, AR=39% and AR=57%. These hardness values higher than that of as drawn

conditions indicates that the aging process is occurring during posterior heat treatment. Higher maximum hardness values for higher area reduction wires means that more nuclei to promote precipitation are created for larger reduction. The respective microstructures of those wires are shown in Figures 2b, 3b and 4b and one can still see the deformed band structure but not the perception of these nucleated particles. The particles precipitation can be seen in samples annealed at 750°C and 850°C being coarser for the second. That is, precipitates coalescence is occurring.

The softening of the wires samples start at 550°C for AR=14% and 39% and at 650°C for AR=57% as seen in Figure 5. This occurrence could be explained in function of the decrease of crystallographic defects and coalescence of precipitates. The Figures 2c, 3c and 4c show well this effect, but there is still deformation bands for AR=14% and 39% compared with AR=57%. In this stage still is occurring the recovery process of the drawn wires because the annealing at low temperatures is not enough to eliminate completely the complex defects created by cold work. The annealing at 850°C marks the beginning of the recrystallization for the three area reductions, reflecting in a large decrease of hardness. From this point the hardness can decrease to about 50%. The particles precipitation are seen in samples annealed at 750°C and 850°C being coarser for the second as seen in Figures 3d and 4d but less in Figure 2d for lower area reduction. The annealing at 950°C promoted the dissolution of practically all particles and microstructure are fully recrystallized as seen in Figure 2(e), Figure 3(e) and Figure 4(e) returning to solution treated condition as shown in Figure 1. As seen in Figure 2e, the microstructure is not homogeneous presenting variation in grain size which is attributed to a low area reduction.

The literature^(1-3,8) reports that the precipitation of second phase particles in Fe-Mn-Si based alloys can improve the SME due to the partitioning effect subdividing the austenite grain in smaller domains and therefore facilitating the forward and backward movement of $\gamma \leftrightarrow \varepsilon$ transformation. In this paper it was not investigated the influence of these particles in the shape recovery but some preliminary results indicate that the annealing at 850°C for AR=57% wire gives the best result in terms of shape recovery. Experiments are underway in order to optimize the thermomechanical processing aiming good shape memory effect and also to identify the particles that appear during post drawing heat treatment.

7 CONCLUSION

From this work some concluding remarks are:

- (1) The solution treated sample presents annealing twins which are characteristic of Fe-Mn-Si based SMA's, that have a low stacking fault energy.
- (2) The hardness increased from about 237 HV of solution treated sample to a maximum of 455 HV for AR=57%, that is almost twice indicating the cumulative effect of work hardening.
- (3) The solution treated sample did not present the hardening effect but the drawn wires had their hardness increased after heat being their maximum of 428HV at 450°C, 522HV at 450°C and 639HV at 550°C

respectively for AR=14%, AR=39% and AR=57%. The hardness increase was attributed to a precipitation of second phase particles.

- (4) The hardness decreased as the heat treatment increased and the second phase particles coalesce and finally at 950°C disappear and all the drawn samples returned to solution treated condition.

Acknowledgements

The authors wish to thank FAPESP (00/09730-1 and 2009/09091-3), CAPES, Universal CNPq (473612/2006-2), MCT/Casadinho CNPq - UFCG/ITA, FINEP, PRO-INFRA, IEAv, AEB and Mineral Technology Center (CETEM).

REFERENCES

- 1 WEN, Y.; PENG, H.; WANG, C.; YU, Q. and LI, N. A novel training-free cast Fe-Mn-Si-Cr-Ni shape memory alloy based on formation of martensite in a domain-specific manner. *Advanced Engineering Materials*. 2011, 13, 48-56.
- 2 WEN, Y.H.; PENG, H.B.; SUN, P.P.; LIU, G. and LI, N. A novel training-free cast Fe-18Mn-5.5Si-9.5Cr-4Ni shape memory alloy with lathy delta ferrite. *Scripta Materialia*. 2010, 62, 55-58.
- 3 YANG, S.Z.; LI, N.; WEN, Y.H. and PENG, H.B. Effect of ageing temperature after pre deformation on shape memory effect and precipitation process of Cr₂₃C₆ carbide in a FeMnSiCrNiC alloy. *Materials Science and Engineering A*. 2011, 529, 201-206.
- 4 JIANG, B.H.; SUN, L.; LI, R. and HSU, T.Y. Influence of austenite grain size on $\gamma \rightarrow \epsilon$ martensitic transformation temperature in Fe-Mn-Si-Cr alloys. *Scripta Metallurgica et Materialia*. 1995, 33, 63-68.
- 5 OTUBO, J.; NASCIMENTO, F.C.; MEI, P.R.; CARDOSO, L.P. and KAUFMAN, M.J. Influence of austenite grain size on mechanical properties of stainless SMA. *Materials Transactions*. 2002, v. 43, n. 5, p. 916-919.
- 6 ROVERE, C.A.D.; ALANO, J.H.; SILVA, R.; NASCENTE, P.A.P.; OTUBO, J.; KURI, S.E. Characterization of passive films on shape memory stainless steels. *Corrosion Science*. 2012, 57, 154-161.
- 7 ROVERE, C.A.D.; ALANO, J.H.; OTUBO, J.; KURI, S.E. Corrosion behavior of shape memory stainless steel in acid media. *Journal of Alloys Compounds*. 2011, 509, 5376-5380.
- 8 AKHONDZADEH, A.; ZANGENEH-MADAR, K. and ABBASI, S.M. Influence of annealing temperature on the shape memory effect of Fe-14Mn-5Si-9Cr-5Ni alloy after training treatment. *Materials Science and Engineering A*. 2008, 489, 267-272.
- 9 STANFORD, N. and DUNNE, D.P. Effect of Si on the reversibility of stress-induced martensite in Fe-Mn-Si shape memory alloys. *Acta Materialia*. 2010, 58, 6752-6762.
- 10 OTUBO, J.; MEI, P. R.; LIMA, N. B.; SERNA, M. M.; GALLEGOS, E. O efeito do tamanho de grão austenítico no número de orientações das variantes de martensita em ligas inoxidáveis com efeito de memória de forma. *REM – Revista Escola de Minas*, Ouro Preto, MG, 60(1): 129-134, jan. mar. 2007.
- 11 ANDRADE, E.C.; KÄFER, K.A.; BERNARDI, H.H.; OTUBO, J. Influência do recozimento na liga Fe-Mn-Si-Cr-Ni-Co com efeito de memória de forma processada por trefilação. 66^o Congresso da ABM, 18 a 22 de Julho, 2011, São Paulo, SP.

- 12 OTUBO, J.; MEI, P.R.; KOSHIMIZU, S.; SHINOHARA, A.H. and SUZUKI, C.K. Relationship between thermomechanical treatment, microstructure and α' martensite in stainless Fe-based shape memory alloys. *Materials Science and Engineering A*. 1999, 273-275, 533-537.
- 13 LI, H.; DUNNE, D. and KENNON, N. Factors influencing shape memory effect and phase transformation behaviour of Fe-Mn-Si based shape memory alloys. *Materials Science and Engineering A*. 1999, 273-275, 517-523.
- 14 YONEYMA, N.; SETODA, T.; KUMAI, S.; SATO, A.; KOMATSU, M. and KIRITANI, M. Structural refinement and strengthening of an Fe-Mn-Si-Cr-Ni shape memory alloy by high-speed rolling. *Materials Science and Engineering A*. 2003, 350, 125-132.
- 15 ASHBROOK, R. W. Jr.; MARDER, A. R. The effect of initial carbide morphology on abnormal grain growth in decarburized low carbon steel. *Metallurgical Transactions A*. 1985, 16, 897-906.
- 16 REED-HILL, R. E. *Princípios de Metalurgia Física*. Editora Guanabara Dois S.A. Rio de Janeiro, 1982, p. 228-232 e 244-253.
- 17 OTUBO, J. *Desenvolvimento de ligas inoxidáveis com efeito de memória de forma: elaboração e caracterização*. FEM/DEMA/UNICAMP, Dezembro de 1996, Campinas, SP. (Tese de Doutorado).
- 18 NASCIMENTO, F.C.; RIGO, O.D.; OTUBO, J.; MEI, P.R. and MOURA NETO, C. Evolução das fases formadas durante tratamentos termomecânicos em ligas inoxidáveis com efeito de memória de forma. *Anais do Congresso Nacional de Engenharia Mecânica - CONEM*, 07 a 11 de Agosto de 2000, Natal, RN.